

FISCHER TROPSCH SYNTHESIS IN SUPERCRITICAL FLUIDS

DE-FG22-92PC92545

QUARTERLY TECHNICAL PROGRESS REPORT

January 1, 1995 - March 31, 1995

Principal Investigators

Aydin AKGERMAN
Dragomir B. BUKUR

Chemical Engineering Department
Texas A&M University
College Station, TX 77843

MASTER

Organization

Texas Engineering Experiment Station
308 Wisenbaker Engineering Research Center
College Station, TX 77843-3124

I. Objectives for the Second Quarter, Year 3:

A. Fischer Tropsch Reaction Related Studies

Our objectives for this quarter were: (1) to install and test the temperature probe and the flammable gas detector: (2) to conduct Fischer-Tropsch experiments at baseline conditions and at a high pressure in order to test the newly constructed fixed bed reactor assembly.

B. Diffusion Coefficients of F-T Products in Supercritical Fluids

Our objectives for this quarter were to verify the results we reported on the molecular diffusion coefficients at the same conditions. This would allow us to verify the accuracy of the results and continue on with the tortuosity calculation. We will determine the tortuosity for this catalyst and thus be able to calculate effective diffusivities from molecular diffusion coefficients without dual experimentation.

This would give us the porosity over tortuosity ratio that relates molecular diffusivities to effective diffusivities. From equation (1) (Wakao and Kaguei, "Heat and Mass Transfer in Packed Beds", Gordon and Breach, New York, 1982) this value is independent of temperature and pressure, thus effective diffusivities can easily be determined from molecular diffusion coefficients without further experimentation.

$$D_{eff} = \frac{\epsilon_p}{\tau} D_m \quad (1)$$

The porosity has been determined from independent experiments. Thus the tortuosity can be determined from the previous ratio.

II. Accomplishments and Problems, Second Quarter, Year 3:

A. Fischer Tropsch Reaction Related Studies

(1) Temperature probe and flammable gas detector

We have installed and used the temperature probe during the shake down run for monitoring the axial temperature profile of the fixed bed reactor. One of the six thermocouples was found malfunctioning. We plan to contact the manufacturer and correct the problem before the next test.

We have also installed and tested the flammable gas detector unit, which consists of a Sensidyne combustible gas transmitter and a Sensidyne Model 1000 single channel controller (Sensidyne Inc., Clearwater, FL), for monitoring propane vapors/gases at concentrations below its lower explosive limit (LEL). The detector was calibrated using a calibration gas containing 1.5 vol % (30 % LEL) methane obtained from Sensidyne, and was adjusted to read directly the equivalent % LEL concentration of propane (55 % LEL of propane) using a conversion factor provided by the manufacturer. The low level alarm on the controller was set at 20 % LEL of propane while the high alarm at 40 % LEL. The high alarm relay contacts were also wired to a solenoid valve installed immediately downstream of the propane tank regulator. In the case of a propane leak when its vapor concentration exceeds the 20 % LEL (0.4 vol % propane) the audible alarm on the detector will sound, and when the propane concentration exceeds the 40 % LEL (0.8 vol % propane), the relay will further activate the solenoid valve to stop the propane flow. The detector reading can be easily converted to % LEL of other gases by respective conversion factors if other supercritical solvents besides propane will be used in the future.

(2) Shake-down run

We have completed a Fischer-Tropsch reaction test during this quarter. The purpose of the experiment was mainly two fold: first, as a shake-down run to test the newly constructed fixed bed reactor assembly; and second, to study the effect of total reaction pressure on catalyst activity and selectivity.

A Ruhrchemie catalyst designated LP 33/81 (Ruhrchemie AG, Oberhausen - Holten, Germany) was used in this test. Catalyst pellets were crushed to 30-60 mesh size and diluted with glass beads of same size prior to loading into the reactor. Details of our fixed bed experimental procedures can be found in Bukur et al. (*Ind. Eng. Chem. Res.*, 1989, 28, 1130-1140). The catalyst was reduced with hydrogen at 220°C, ambient pressure and a flowrate of 5100 cc/min (which corresponds to linear superficial velocity of 150 cm/s) for 1 h. Then it was tested at baseline reaction conditions of 250°C, 200 psig, 2.0 NI/g-cat/h and H₂/CO ratio of 0.67 for the first 140 h on stream. After that, the total reaction pressure was increased to 1000 psig using nitrogen as a balance gas while keeping the syngas partial pressure and space

velocity the same as at the baseline conditions (i.e., $P(\text{H}_2+\text{CO}) = 200$ psig, $P(\text{N}_2) = 800$ psig). Testing at high pressure lasted for another 145 h, followed by establishment of the baseline conditions at 288 h on stream. This test (FA-3143) was terminated voluntarily after 320 h on stream, and results from four mass balances, two each at the baseline conditions and at high reaction pressure conditions, are reported in Table 1.

Changes in catalyst activity, measured in terms of (H_2+CO) conversion, and stability with time on stream (TOS) and total reaction pressure are illustrated in Figure 1. The catalyst was fairly stable with time at the baseline conditions. The steady state values of (H_2+CO) and CO conversion were about 59 %. The H_2/CO usage ratio was similar to the feed ratio, about 0.67.

After increasing reaction pressure to 1000 psig using nitrogen (N_2) as balance gas, we had experienced some experimental problems. Due to high gas flow rate a low pressure cold trap was unable to condense all liquid products. During the two mass balances at 1000 psig, only a small amount of organic phase products and hardly any aqueous phase products were collected in the cold trap. Consequently, the total mass balance closures for these two balances were relatively low (96.5 and 98.7%), and hydrocarbon selectivity could not be determined accurately. Uncondensed liquids were carried by the tail gas stream to an on-line gas chromatograph (Carle 400 Series) causing problems with gas analysis (introduction of additional peaks, baseline drift). The presence of large amount of nitrogen resulted in dilution of product concentrations, which also had some effect on the accuracy of gas analysis.. The syngas flow rate drifted slightly from the expected value, based on a mass flowafter calibration before the test, during operation at high pressure. Problems in gas analysis and flow rate caused some fluctuations in the (H_2+CO) conversion measurements, as shown in Figure 1. Nevertheless, the average (H_2+CO) conversion was about 58 %, which is nearly the same as that at the baseline conditions. Therefore, the catalyst activity was not affected by increase in total pressure. The (H_2+CO) conversion increased to about 65 % after returning to the baseline conditions during the last part of the experiment, and the usage ratio was about 0.64 (A smaller usage ratio is indicative of higher water-gas-shift activity). We have observed similar increases of activity with TOS in our previous tests with the Ruhrchemie catalyst.

Hydrocarbon product distribution shifted gradually towards low molecular weight products with TOS. The average values from the two mass balances at the baseline conditions (TOS = 67 and 116 h) were: $C_1 = 7.4$ wt%, $C_2-C_4 = 18.7$, $C_5-C_{11} = 26.0$ and $C_{12}+ = 47.9$ %. During testing at 1000 psig, with N_2 as balance gas, the selectivity of methane increased to 8.6 wt %, C_2-C_4 to 21.0 %, C_5-C_{11} 34.9 %, whereas $C_{12}+$ selectivity decreased to 35.5 %. It should be noted that selectivity results reported here as well as in Table 1 for high pressure conditions represent values after adjustments, compensating for the loss of liquid products. Olefin selectivity and 2-olefin selectivity as a function of carbon number up to C_{15} are plotted in Figures 2 and 3, respectively. The olefin and 2-olefin selectivities were not affected by changes in total reaction pressure and remained stable with time on stream. This indicates that the increase in reaction pressure and the presence of diluent gas, while maintaining the syngas partial pressure and space velocity constant, do not have effect on the adsorption of H_2 and olefins on the catalyst surface, and diffusion rates of reactants and products inside the catalyst pores.

Methane selectivity was about 8.1 wt% after returning to the baseline conditions. The gas chromatograph used for organic products analysis was out of order at this time, therefore, hydrocarbon selectivity data for this period were not determined (TOS = 290-360 h).

In summary, the reactor assembly performed basically well according to the design. Introduction of nitrogen as a balance gas did not have effect on the catalyst activity and selectivity under the conditions studied. To alleviate problems related to products collection encountered during operation at high pressure (i.e., at high gas flow rates) we will make a new low pressure (glass) trap with a larger heat exchange area and longer gas residence time. Also we will add another trap before the on-line GC to collect any uncondensed liquid products, in order to reduce problems with gas analysis in the presence of C_{6+} liquid hydrocarbons.

B. Diffusion Coefficients of F-T Products in Supercritical Fluids

We previously had reported on the methodology to extract molecular diffusion coefficients from experimental data in Taylor dispersion at high temperatures. This methodology has been verified to be accurate by repetition of experimentation. Experiments were not only repeated but also we were able to complete new runs at the same temperature

conditions and a new pressure of 1200 psi.

The experimental data has been analyzed and the results are shown in Table 5. The results show that it seems as if the ratio of tortuosity to porosity is approximately constant and equal to 9 (see Figure 13). The molecular diffusion coefficient and effective diffusivity have the trend of decreasing with increasing density, this follows previous trends we have seen. This trend is displayed in Figures 10-12. Another result which we have found is the effect of flow rate on the diffusion coefficient. Diffusion coefficient should not change with the flow rate or velocity. However, from Figure 9, it can be seen that there is a certain flow rate at which above the system does not perform correctly. This shows the need to follow the design criteria (see quarter 4, year 2) conservatively. For the displayed system the design criteria gave a maximum flow rate corresponding to a residence time of 360 seconds. As seen, all measurements below this flow rate gave consistent results where the results above this rate were less than desirable.

III. Plans for the Third Quarter, Year 3.

A. Fischer Tropsch Reaction Related Studies

(1). complete the safety report for the experimental apparatus and submit it for approval; (2). make modifications of the reactor assembly (product collection traps); (3). make the Fischer-Tropsch test with propane as a supercritical solvent.

B. Diffusion Coefficients of F-T Products in Supercritical Fluids

We will measure the molecular diffusion coefficients and effective diffusivities at more conditions to get a better understanding of the exact value of the tortuosity to porosity ratio. We will determine the tortuosity for this catalyst and thus be able to calculate effective diffusivities from molecular diffusion coefficients without dual experimentation. We then will attempt to find a model to predict the molecular diffusion coefficients to a high degree of accuracy so we may be able to predict both the molecular diffusion coefficient and thus the effective diffusivity a priori.

Table 1. Experimental Conditions for Run FA-2984^a.

Period	Time on Stream h	P _{total} psig	P _{H₂+CO} psig	P _{hexane} psig	(H ₂ +CO) Feed Rate		Hexane Feed Ncc/min
					NL/g-cat/hr	Ncc/min	
0	24 to 68	200	200	0	2.0	100	
3	69 to 192	550	200	350	2.0	100	1.02
4	193 to 237	410	200	210	2.0	200	0.61
5	238 to 300	550	400	150	4.0	100	0.44
6	322 to 358	200	200	0	2.0	100	

a. The reaction temperature and H₂ to CO feed ratio were maintained at 250°C and 0.67, respectively.

Table 2. Summary of Results, Run FA-2984.

Period	0	3	4	5	6
TOS, h	150	187	237	283	360
SV of (H ₂ +CO), NL/g-cat/hr	2.0	2.0	2.0	4.0	2.0
Total pressure, psi	200	550	410	550	200
Type of operation	normal FT	SFT with hexane	FT with hexane	SFT with hexane	normal FT
H ₂ conv, %	63.0	65.0	57.7	55.2	59.5
CO conv, %	57.9	66.0	58.1	42.9	58.0
(H ₂ +CO) conv, %	59.9	65.6	57.9	47.7	58.6
H ₂ /CO usage ratio	0.70	0.64	0.64	0.83	0.66
Mol% ^a CH ₄	5.89	6.57	6.79	7.00	6.27
Mol% ^a C ₂ -C ₄	18.8	10.4	10.7	23.1	21.0
Mol% ^a C ₅ ⁺	75.4	83.0	82.5	69.9	72.7
k, mmol/g-Fe/hr/MPa	207	279	238	173	206

a. from gas phase composition analysis.

Table 3. Experimental Conditions for Run FA-3194a.

Period	Time on Stream hr	P _{total} psi	Type of Operation	(H ₂ +CO) Feed Rate Ncc/min	Solvent Feed Rate Ncc/min
1	23 to 160	750	SFT with propane	150	225 (gas)
3	168 to 265	300	normal FT	150	
4	267 to 335	480	SFT with hexane	150	0.52 (liquid)
6	336 to 355	300	normal FT	150	

a. The reaction temperature, H₂ to CO feed ratio, synthesis partial pressure and synthesis feed rate were maintained at 250°C, 0.67, 300 psi and 3 NL/g-cat/hr, respectively.

Table 4. Summary of Results, Run FA-3194.

Period	1	3	4	6
TOS, h	64	210	320	350
Total pressure, psi	750	300	480	300
Type of operation	SFT with propane	normal FT	SFT with hexane	normal FT
H ₂ conv, %	68.2	54.6	48.5	46.0
CO conv, %	79.4	61.4	58.4	55.7
(H ₂ +CO) conv, %	74.9	58.7	54.5	51.9
H ₂ /CO usage ratio	0.57	0.59	0.55	0.56
Mol% ^a CH ₄	4.67	4.46	4.17	4.43
Mol% ^a C ₂ -C ₄	20.3	21.1	18.0	20.1
Mol% ^a C ₅ ⁺	75.0	74.5	77.8	75.4
k, mmole/g-Fe/hr/MPa	313	188	192	170

a. from gas phase composition.

DISCLAIMER

This report was prepared as an account of work sponsored by an agency of the United States Government. Neither the United States Government nor any agency thereof, nor any of their employees, makes any warranty, express or implied, or assumes any legal liability or responsibility for the accuracy, completeness, or usefulness of any information, apparatus, product, or process disclosed, or represents that its use would not infringe privately owned rights. Reference herein to any specific commercial product, process, or service by trade name, trademark, manufacturer, or otherwise does not necessarily constitute or imply its endorsement, recommendation, or favoring by the United States Government or any agency thereof. The views and opinions of authors expressed herein do not necessarily state or reflect those of the United States Government or any agency thereof.

Table 5.

Experimental Results

T (K)	P (psia)	Density (g/cm ³)	D _{eff} * 10 ⁺⁰⁸ (m ² /s)	D _{ab} * 10 ⁺⁰⁸ (m ² /s)	τ/ε
523	900	0.04569	0.923 ± 0.20	7.03 ± 0.246	7.62 ± 1.51
533	900	0.04460	0.803 ± 0.14	6.91 ± 0.240	8.60 ± 1.87
543	900	0.04357	0.742 ± 0.18	6.70 ± 0.278	9.03 ± 2.03
523	1200	0.06192	0.650 ± 0.18	6.10 ± 0.990	9.38 ± 2.45
533	1200	0.06034	0.610 ± 0.15	5.90 ± 0.660	9.66 ± 1.94
543	1200	0.05885	0.520 ± 0.15	6.00 ± 0.450	10.88 ± 1.83
523	1500	0.07839	0.498 ± 0.10	4.99 ± 0.606	10.01 ± 4.88
533	1500	0.07626	0.488 ± 0.20	5.71 ± 0.668	11.70 ± 3.06
543	1500	0.07428	0.692 ± 0.21	6.29 ± 0.734	9.09 ± 2.14

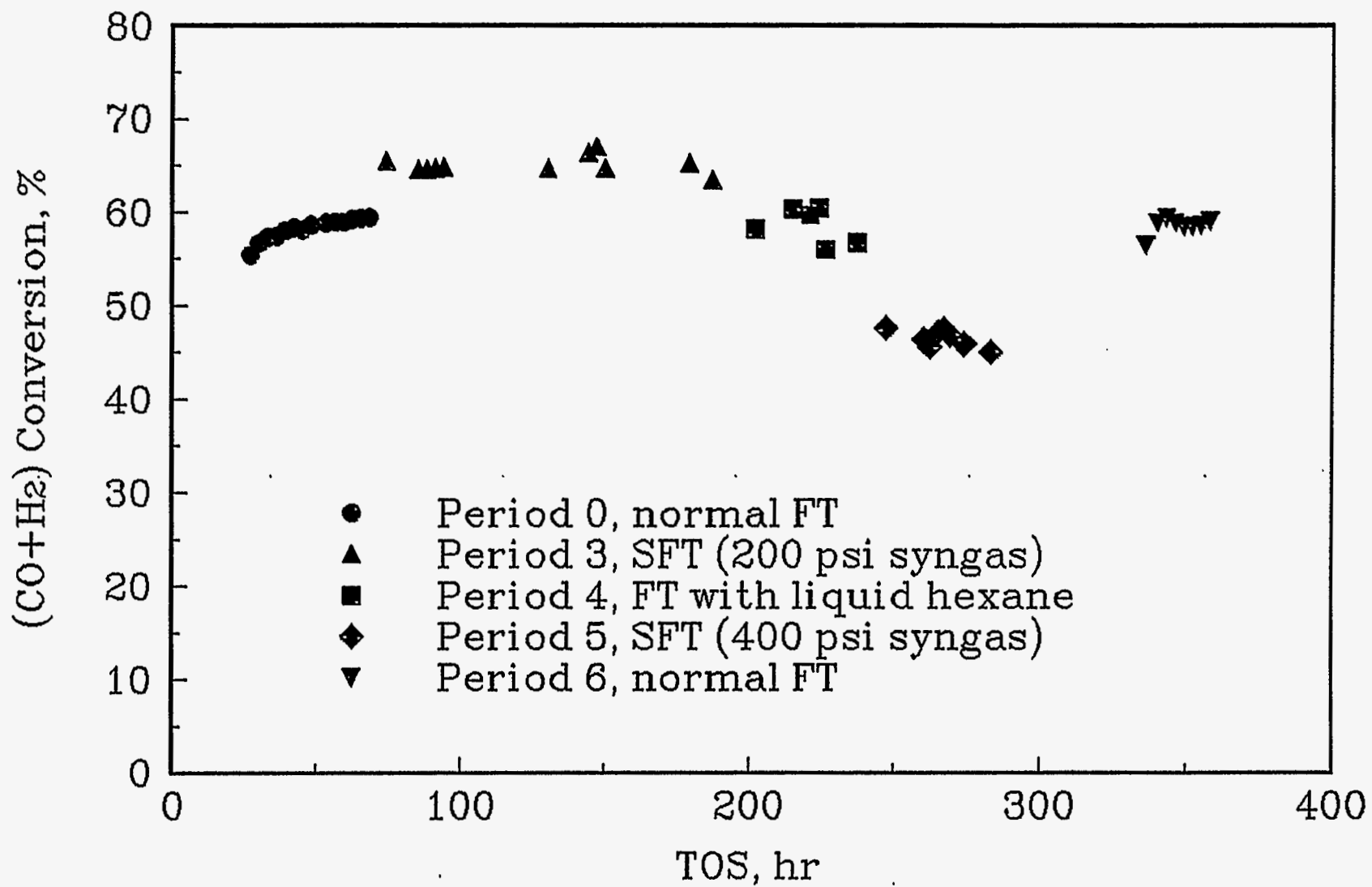


Figure 1. Variation in synthesis gas conversion with process conditions and time on stream during Run FA-2984.

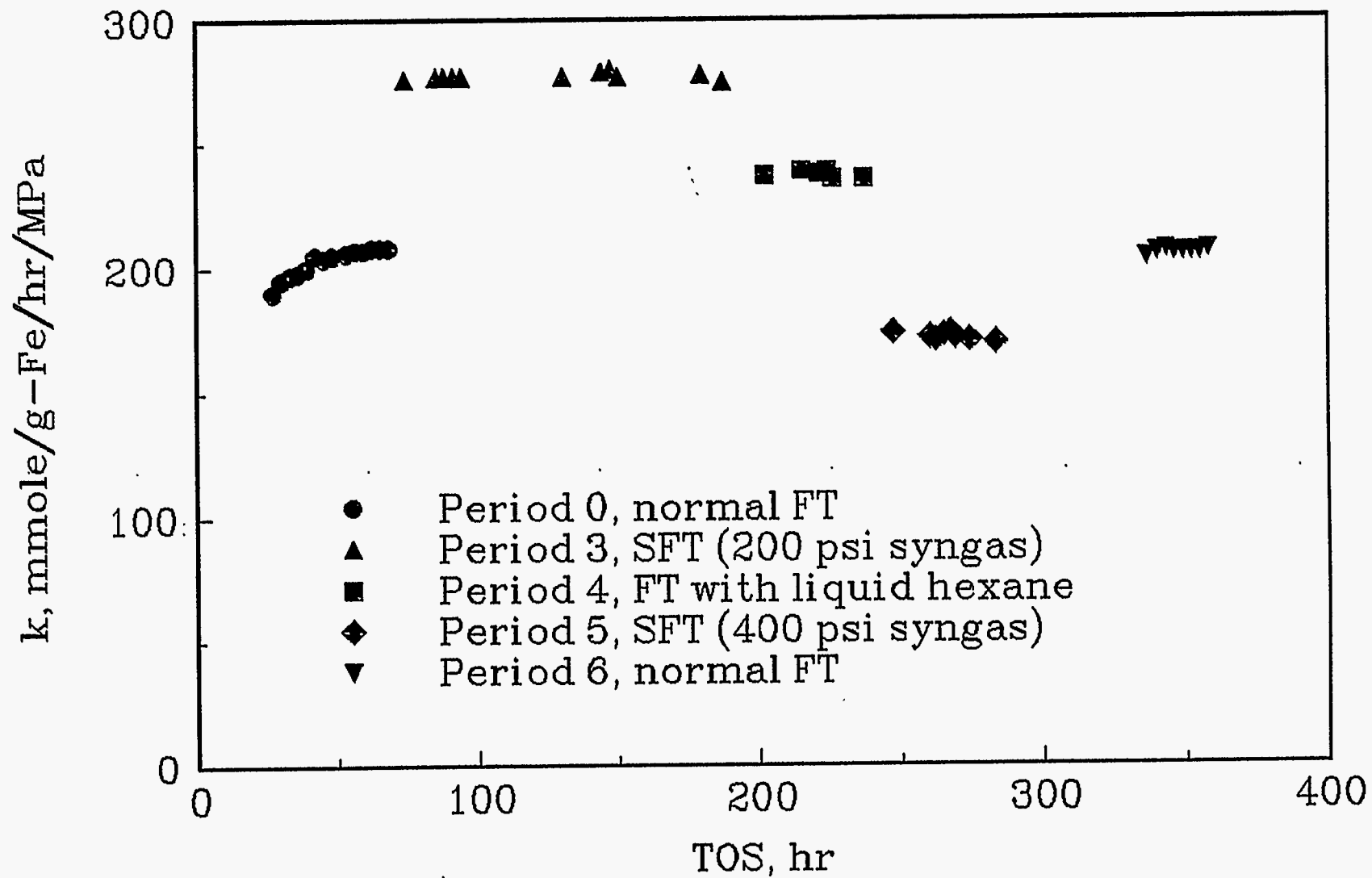


Figure 2. Variation in apparent reaction rate constant with process conditions and time on stream during Run FA-2984.

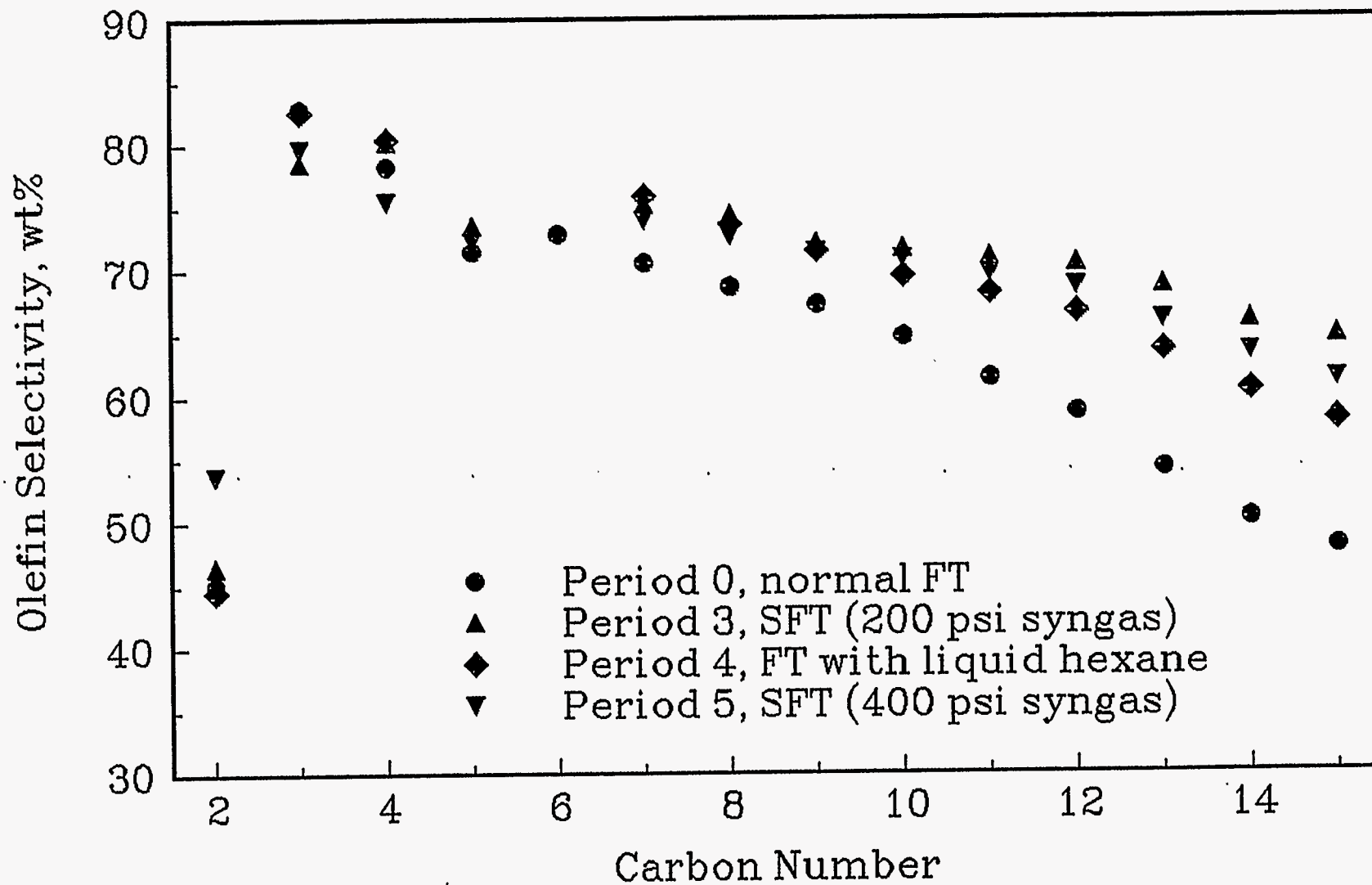


Figure 3. Olefin selectivities during different periods of Run FA-2984.

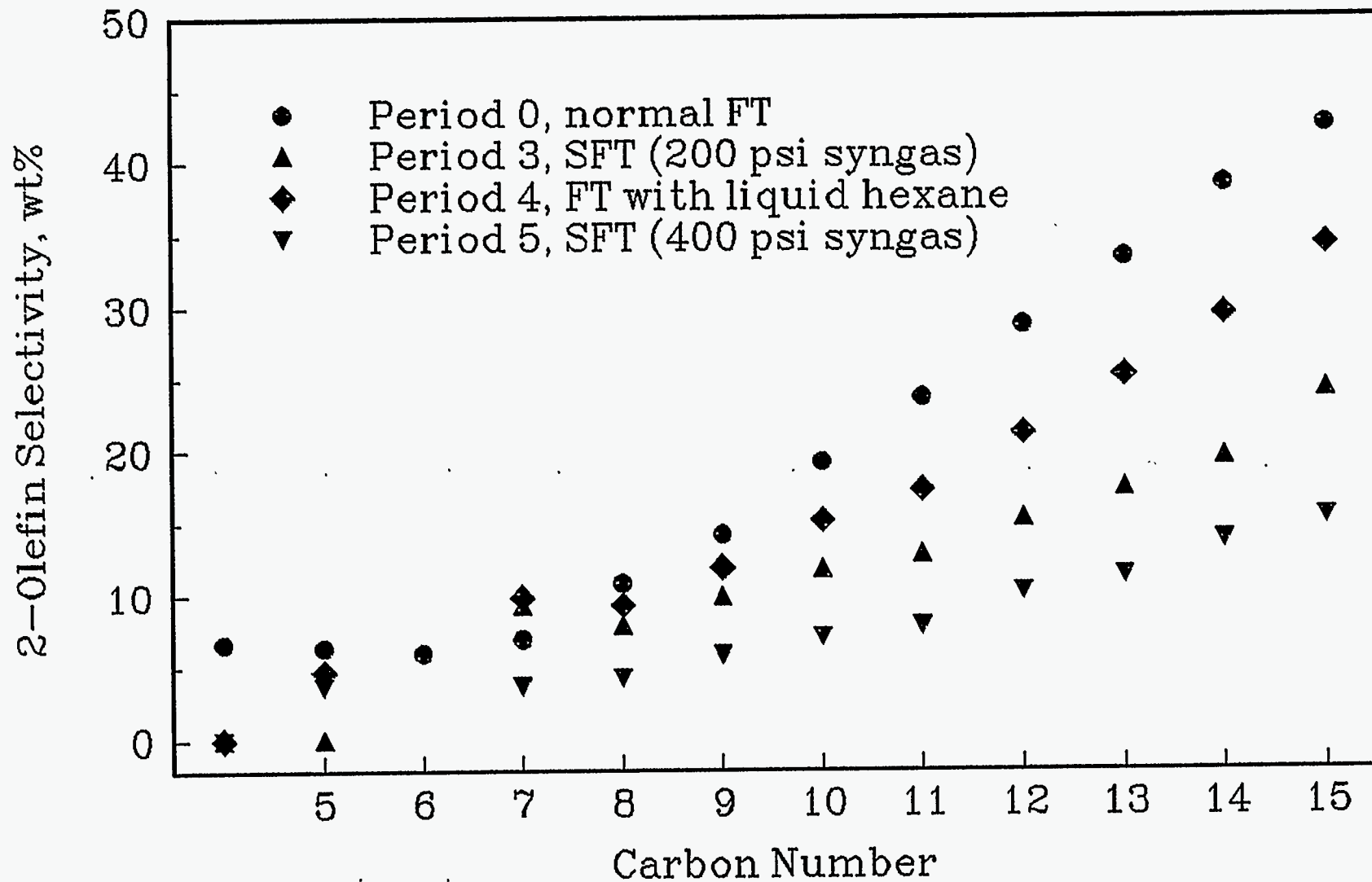


Figure 4. 2-olefin selectivities during different periods of Run FA-2984.

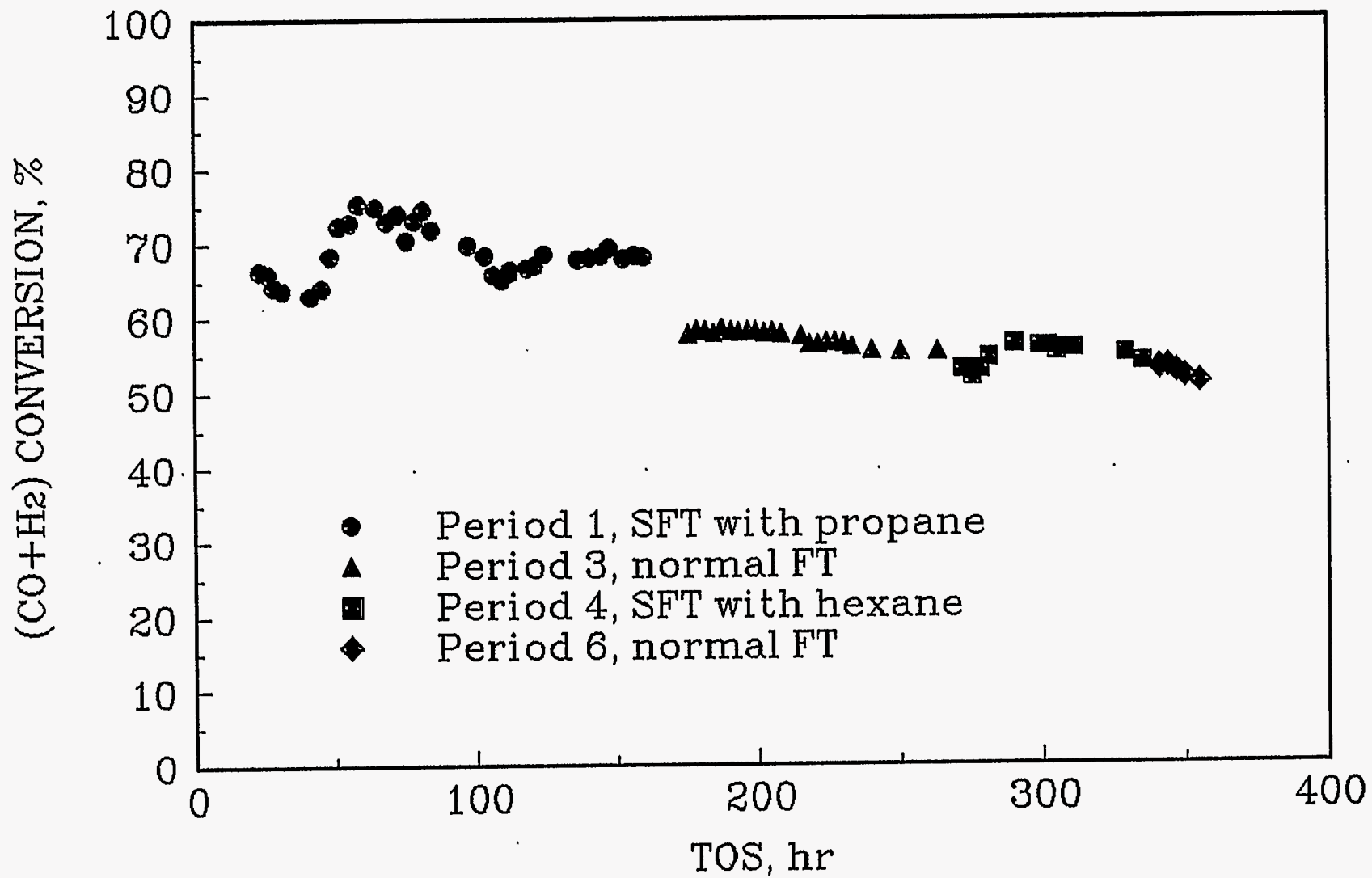


Figure 5. Variation in synthesis gas conversion with process conditions and time on stream during Run FA-3194.

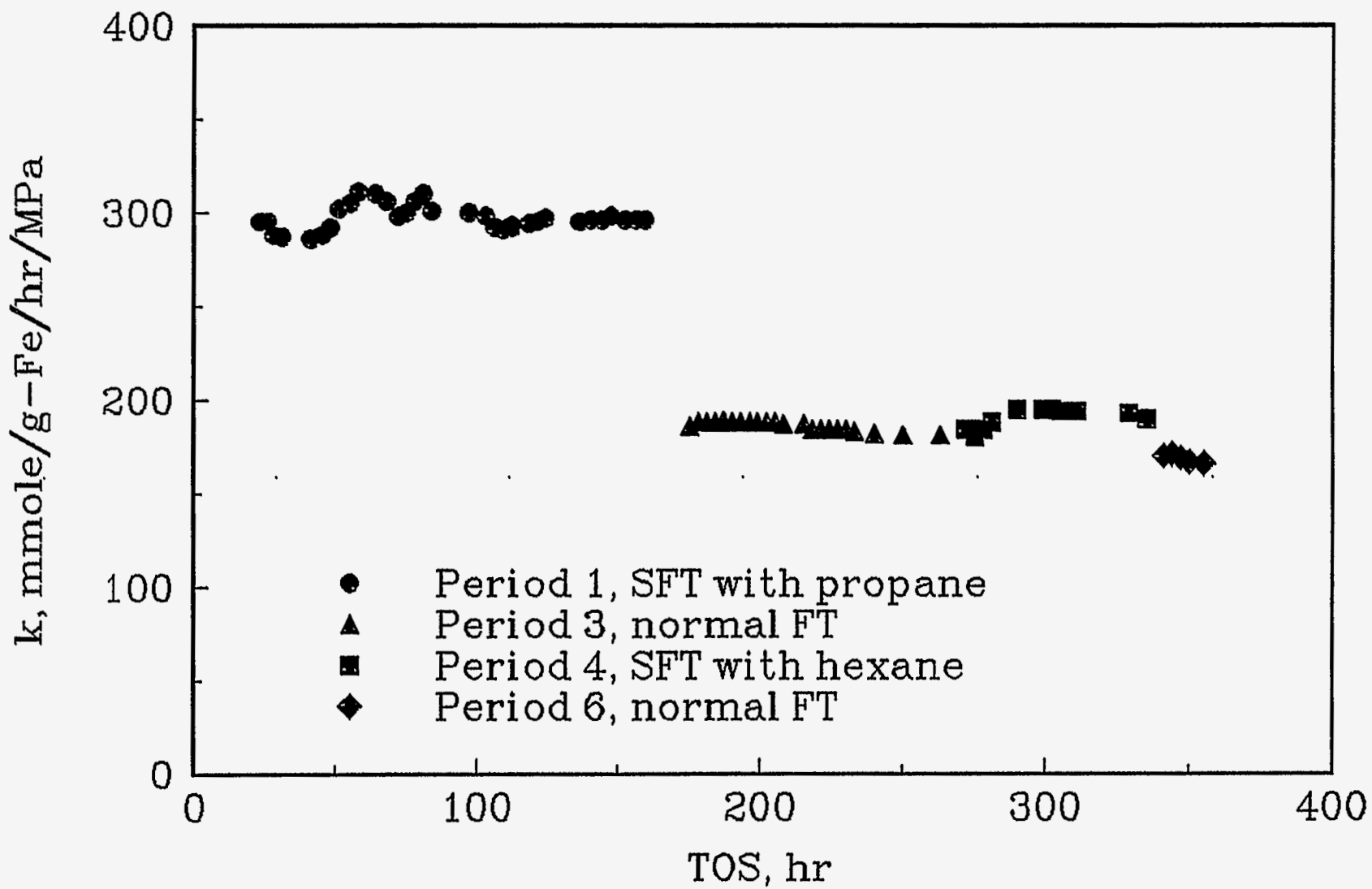


Figure 6. Variation in apparent reaction rate constant with process conditions and time on stream during Run FA-3194.

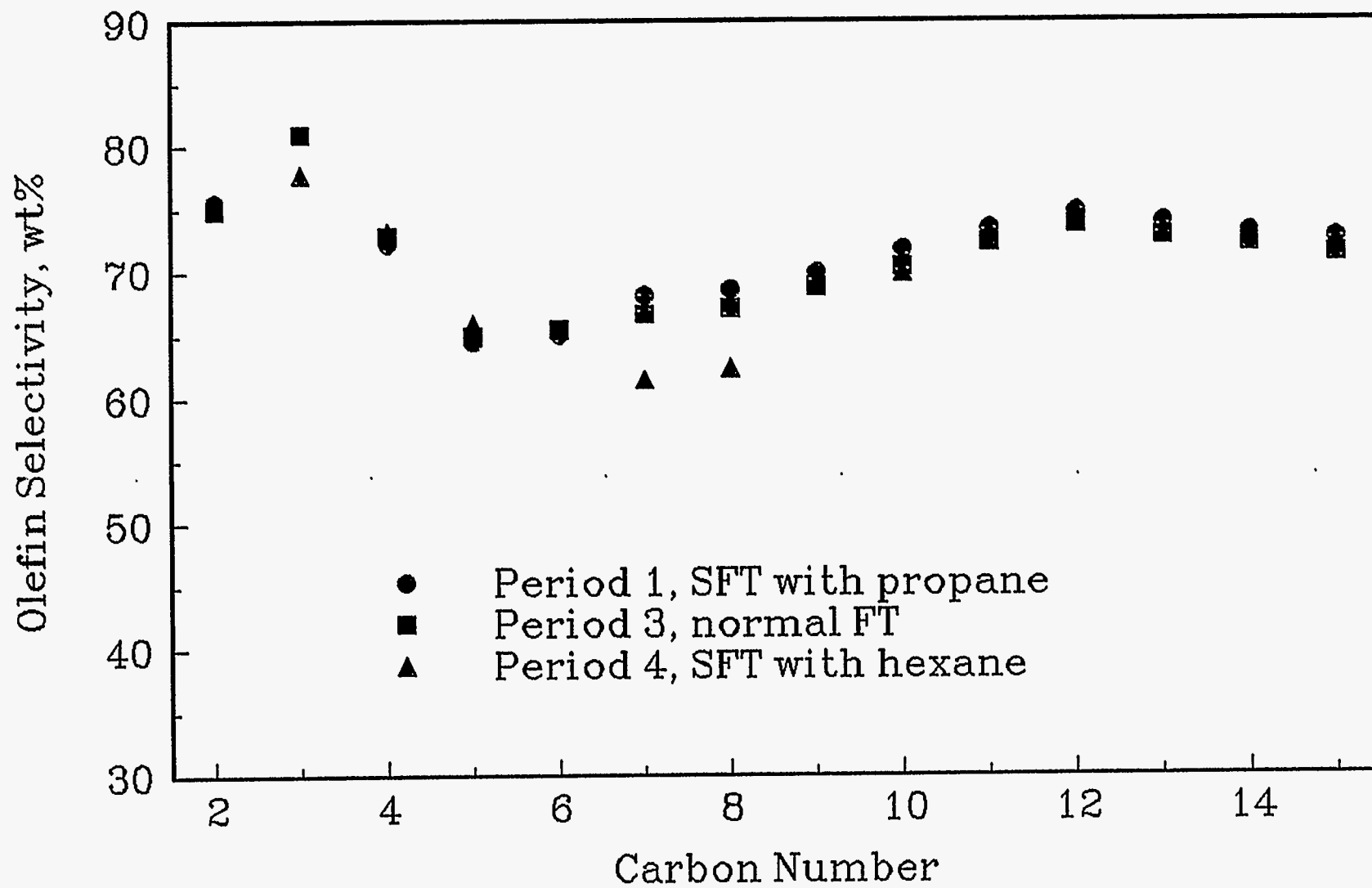


Figure 7. Olefin selectivities during different periods of Run FA-3194.

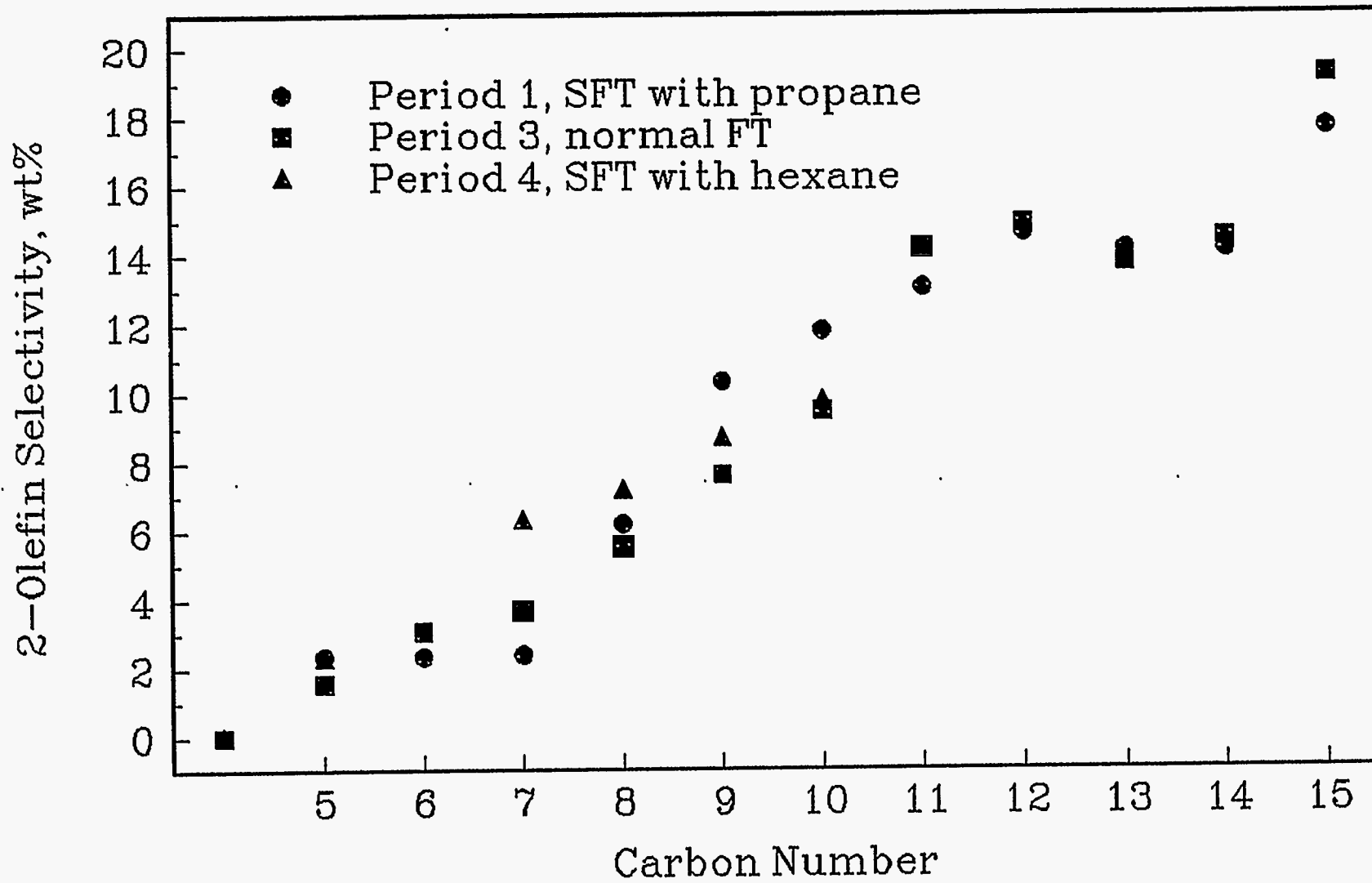


Figure 8. 2-olefin selectivities during different periods of Run FA-3194.

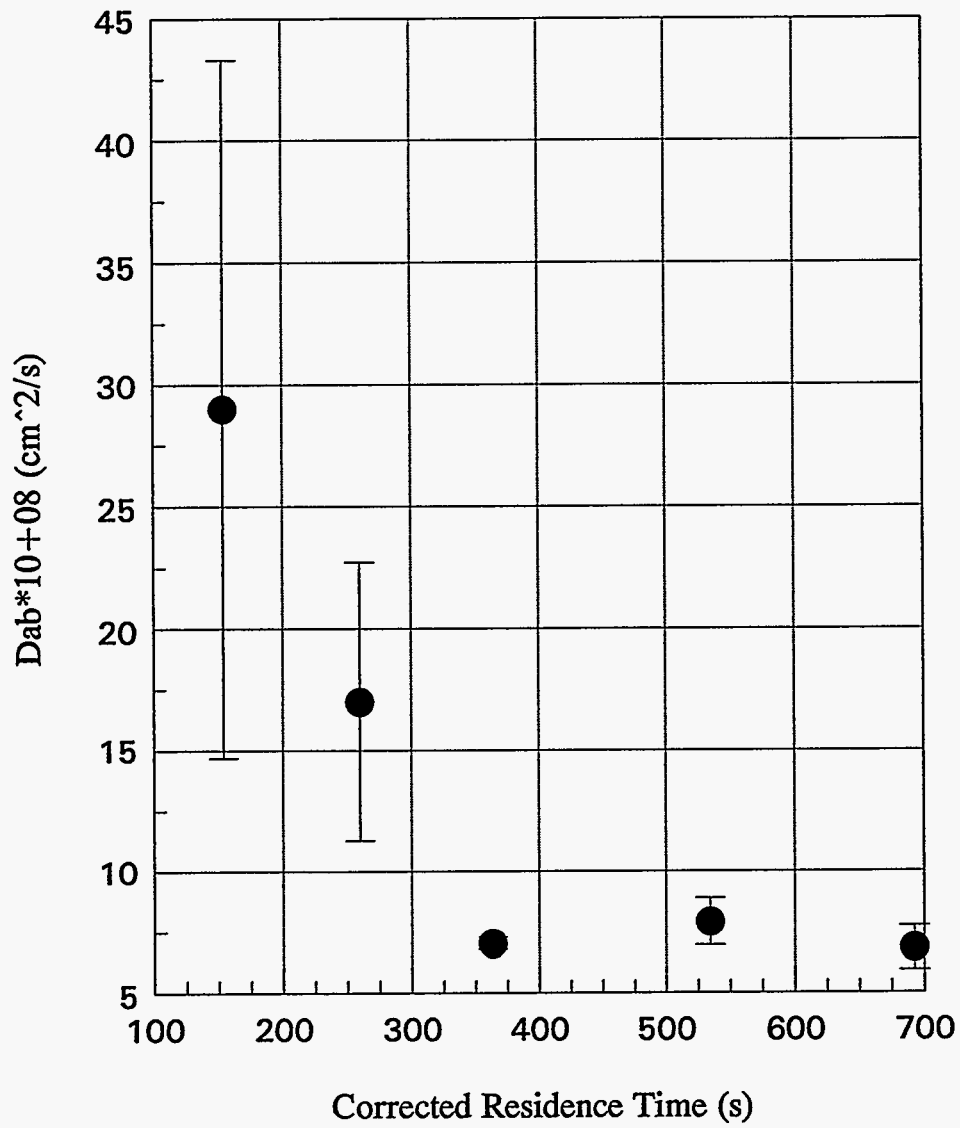


Figure 9. Diffusion Coefficient at T=523K P=900psia

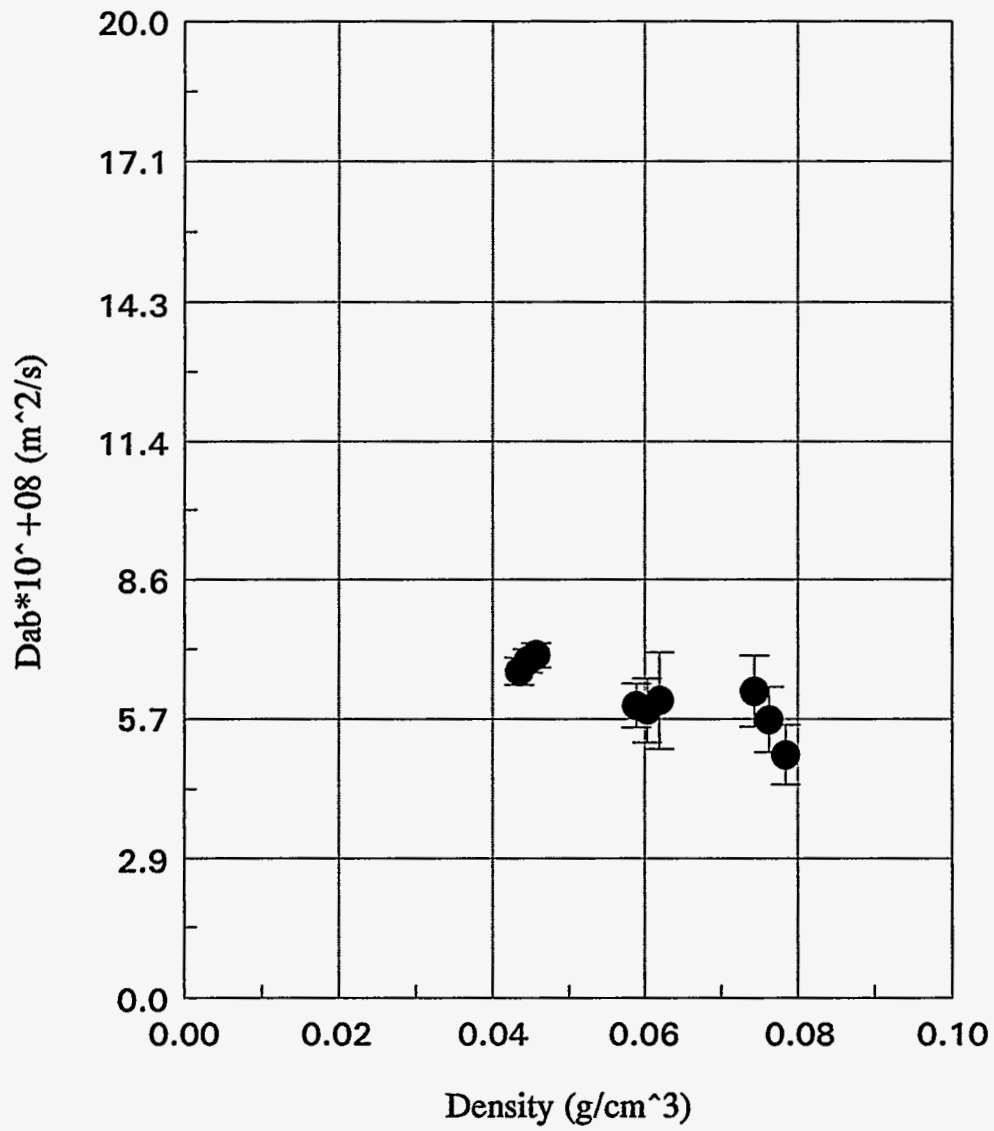


Figure 10. Trend of Dab with Density

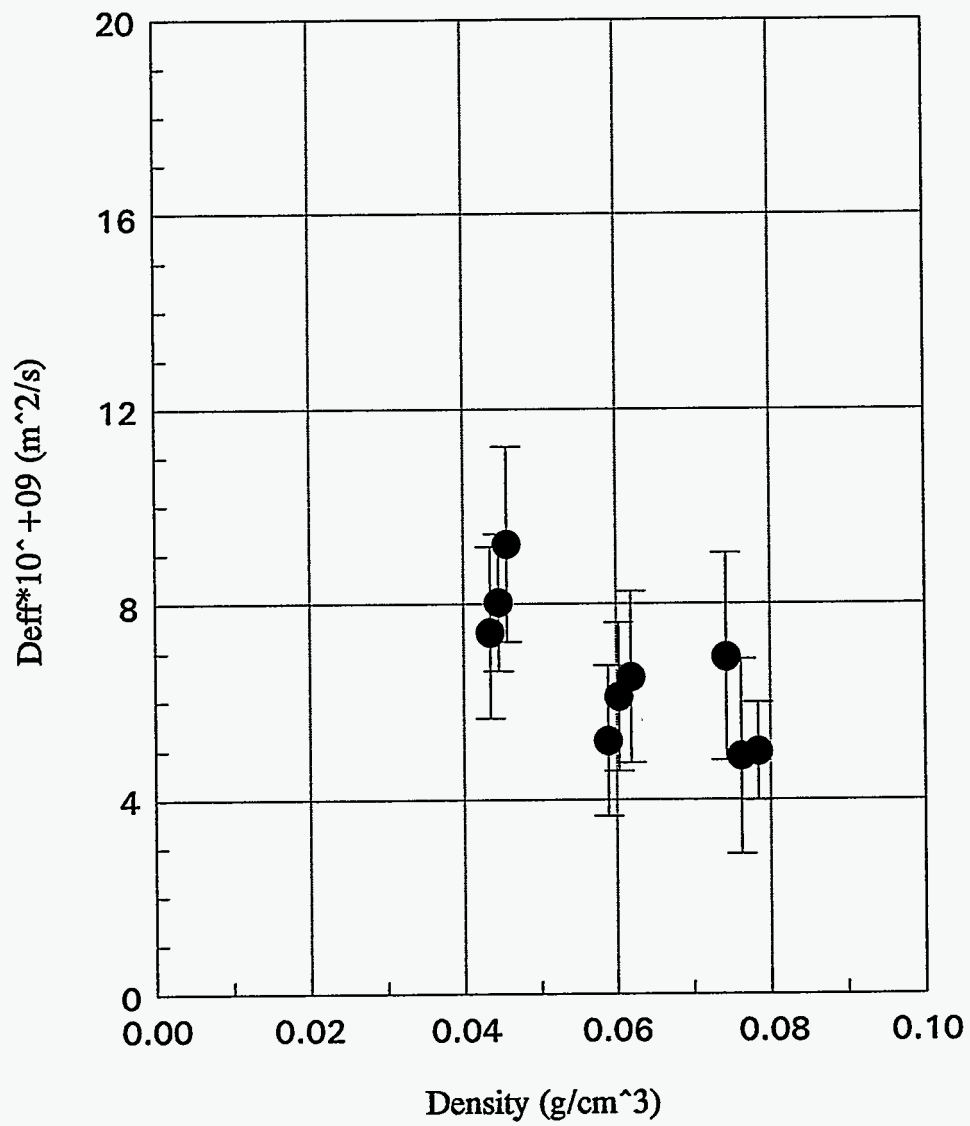


Figure 11. Trend of Deff with Density

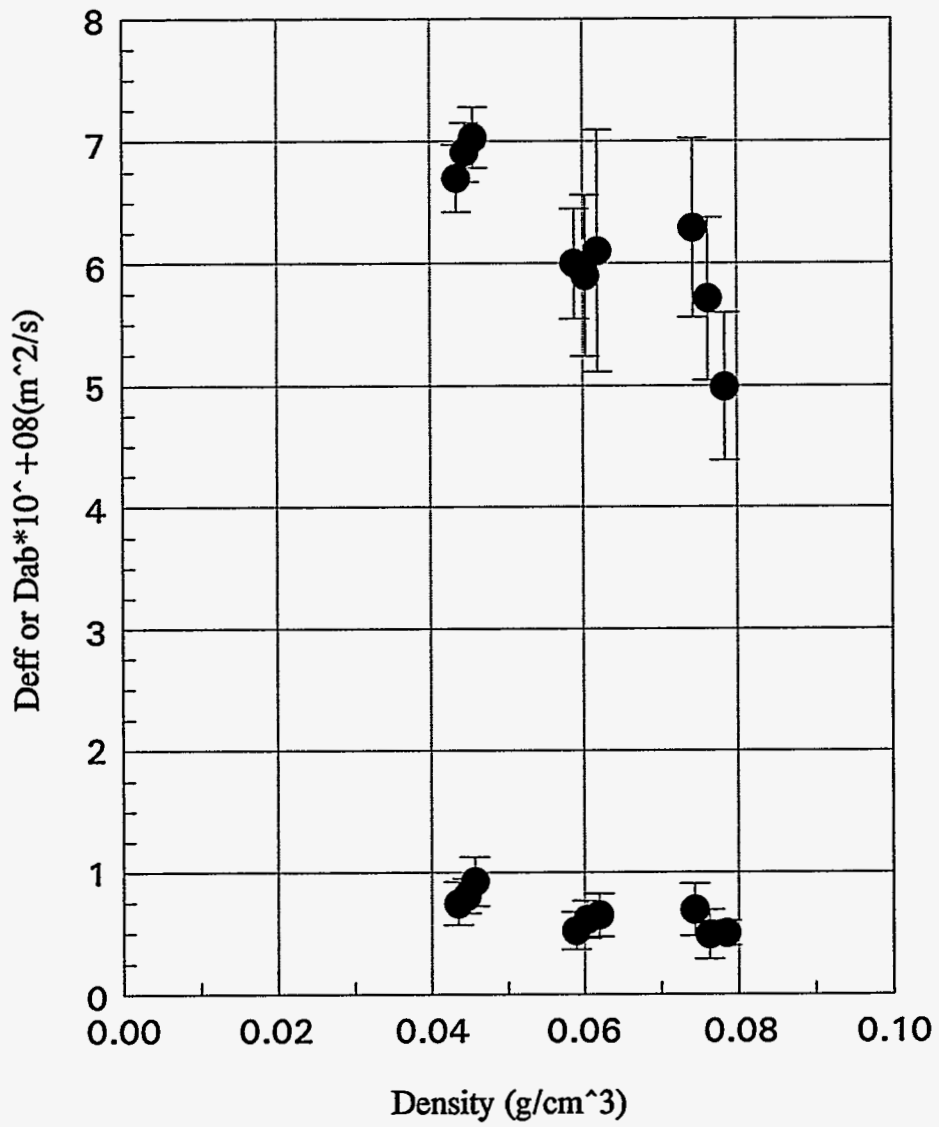


Figure 12. Trend of Deff or Dab with Density

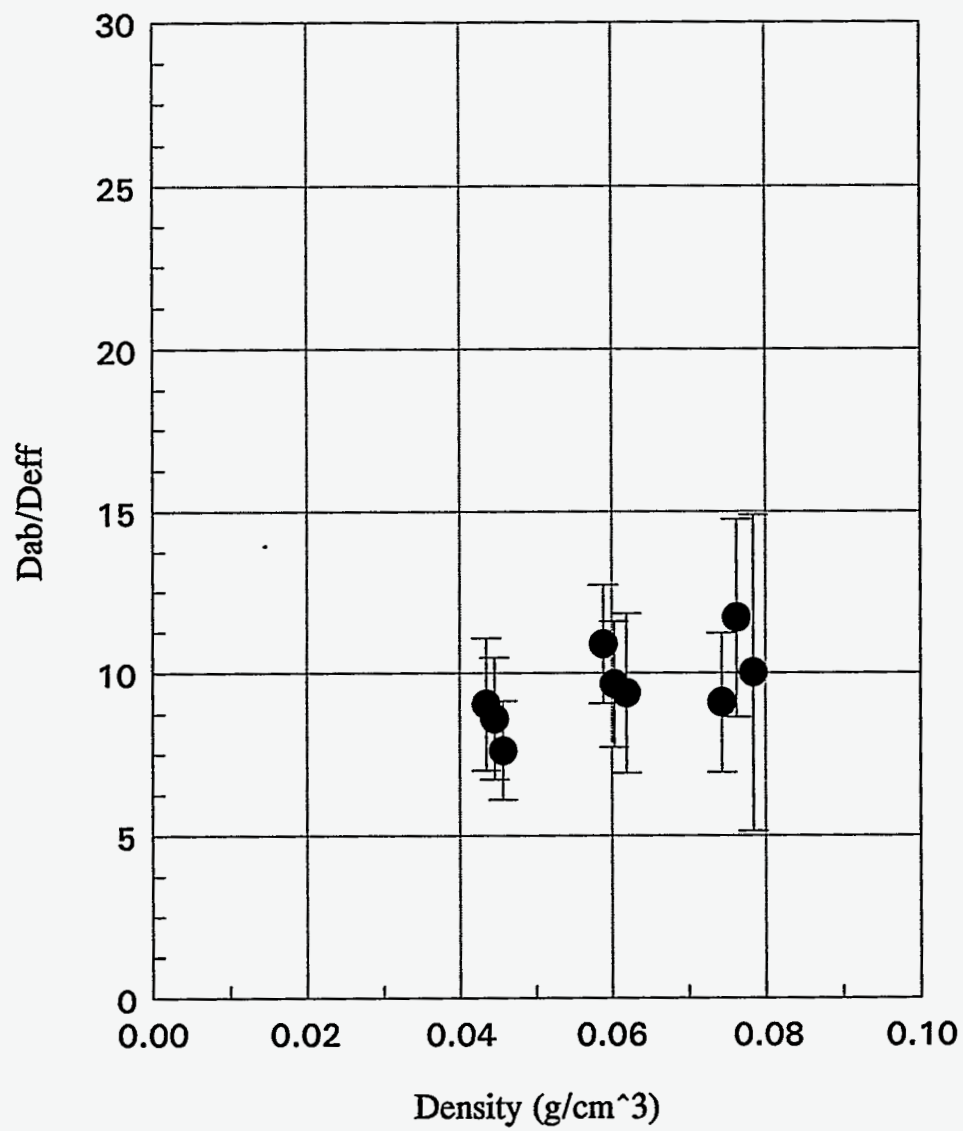


Figure 13. Trend of (Dab/Deff) with Density